TECHNICAL ARTICLE

Synthesis and crystal structures of two novel triazolopyridine compounds solved by local L.S. minimizations from powder diffraction data

Oriol Vallcorba,[1,a),b)] Rosa Adam,[2] Jordi Rius,[1] Rafael Ballesteros,[2] José M. Amigó,[3] and Belén Abarca[2]
[1]*Institut de Ciència de Materials de Barcelona, CSIC, Campus de la UAB, 08193 Bellaterra, Catalunya, Spain*
[2]*Departamento de Química Orgánica, Facultad de Farmacia, Universidad de Valencia, Avenida Vicente Andrés Estelles s/n, 46100 Burjassot, Valencia, Spain*
[3]*Departamento de Geologia, Facultad de Biológicas, Universidad de Valencia, C/ Dr. Moliner s/n, 46960 Burjassot, Valencia, Spain*

(Received 9 January 2014; accepted 7 March 2014)

The heteroaryl-substituted triazolopyridines 3-phenyl-7-(pyrazin-2-yl)-[1,2,3]triazolo[1,5-a]pyridine (**2**) and 3-[6-(pyridazin-3-yl)-pyridin-2-yl]-[1,2,3]triazolo[1,5-a]pyridine (**4**) have been synthesized and characterized (by HRMS, IR, ^{1}H and ^{13}C NMR, XRPD, melting point). The crystal structures have been solved from laboratory powder X-ray diffraction data with the direct-space strategy TALP for molecular compounds based on fast local least-squares minimizations. The crystal structure confirmed the formation of the tridentate compound **4** from a ring chain isomerization process. The almost planar arrangement of atoms in both the structures favors the presence of intermolecular π–π interactions, although weak C–H···N electrostatic interactions seem to be also important for the stabilization of the structure. Powder diffraction data have also proved to be sensible enough to determine the relative rotations of the six-membered rings despite the weak difference in scattering power between C and N atoms. © *2014 International Centre for Diffraction Data*.
[doi:10.1017/S0885715614000402]

Key words: powder diffraction, direct-space methods, TALP, organic compounds, triazolopyridine

I. INTRODUCTION

[1,2,3]Triazolo[1,5-*a*]pyridines **1** (Jones and Abarca, 2010) are heterocyclic aromatic scaffolds that have been shown to be extremely efficient for the preparation of 6,6′-disubstituted-2,2′-bipyridines (Jones *et al.*, 1997), terpyridine-like compounds (Ballesteros-Garrido *et al.*, 2009), and a large amount of 2,6-disubstituted pyridines (Jones and Sliskovic, 1980; Jones *et al.*, 1985). Aryl- or heteroaryl-substituted triazolopyridines present intense fluorescence (Abarca *et al.*, 2006) and coordination properties (Battaglia *et al.*, 1994; Ballesteros *et al.*, 1999; Niel *et al.*, 2003; Arcís-Castillo *et al.*, 2013). These properties have been used in the last years for the preparation of sensors of biologically relevant cations as Zn^{2+} and anions as cyanide or nitrite (Chadlaoui *et al.*, 2006; Ballesteros-Garrido *et al.*, 2012). We are interested in the development of new triazolopyridinic systems containing diazine rings in order to access to fluorescent tridentate ligands. With this idea we have designed the new compounds 3-phenyl-7-(pyrazin-2-yl)-[1,2,3]triazolo[1,5-*a*]pyridine (**2**) and 7-(pyridazin-3-yl)-3-pyridin-2-yl-[1,2,3]triazolo[1,5-*a*]pyridine (**3**) (Figure 1).

On the particular behavior of compounds **1**, regioselective lithiation at the seven-position results as the most powerful strategy to access multi-dentate compounds (Jones and Sliskovic, 1982; Abarca *et al.*, 2004). The preparation of compounds **2** and **3** was tried by means of direct metalation with BuLi at C7, followed by trapping with pyrazine or pyridazine. Electron-deficient aromatic nitrogen-based compounds (pyridines, pyridazines, etc.) trend to accept nucleophilic attack on the alpha position to the nitrogen leading to adducts that can be rearomatized by simple oxidation with $KMnO_4$ (Kress, 1979).

It is important to remark that in compound **1b** (and thus in **3**) a ring chain isomerization takes place (Abarca *et al.*, 2005). This particular feature allows the preparation of a tridentate compound **4** instead of **3**. Once the substituent has been introduced at position 7 (structure **3**), the triazole ring opens and recloses back by the nitrogen less electron poor, the one from the pyridine ring. This affords the tridentate structure 3-[6-(pyridazin-3-yl)-pyridin-2-yl]-[1,2,3]triazolo[1,5-*a*]pyridine (**4**).

^{1}H and ^{13}C NMR spectroscopic data of compound **2** are consistent with the structure of a 3,7-disubstituted triazolopyridine. In contrast, compound **4** has a structure of a 2,6-disubtituted pyridine. Structure **3** (containing a monosubstituted pyridine) should afford one signal of the hydrogen atom in C6′ position. The common chemical shift and coupling constant for this kind of signals are around 8.5–9.0 ppm and 4–5 Hz. In the spectrum, this signal is not observed. However, signals from a three-substituted triazolopyridine, like a hydrogen in C7 position, are observed. This clearly indicates the presence of rearranged compound **4** (Abarca *et al.*, 2005). In order to add more evidences of the proposed structures, X-ray diffraction (XRPD) reveals as the most suitable and powerful technique. In this case, we used powder X-ray diffraction. This technique has provided good results with similar molecules (Adam *et al.*, 2013).

[a)]Author to whom correspondence should be addressed. Electronic mail: ovallcorba@icmab.es
[b)]Current affiliation: CELLS-ALBA Synchrotron Light Facility, 08290 Cerdanyola del Vallès, Barcelona (Spain).

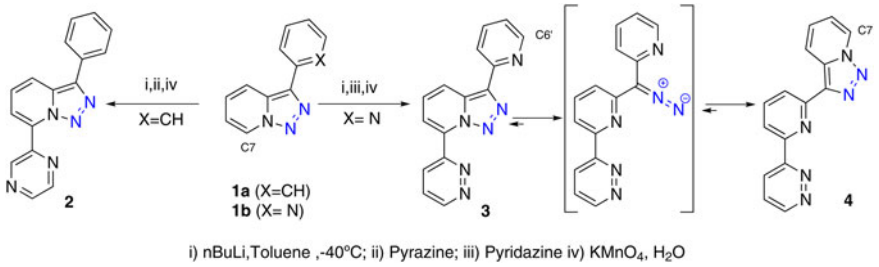

Figure 1. (Color online) Chemical structures and synthesis attempts of compounds **2**, **3,** and **4**.

The crystal structures of **2** and **4** have been solved from X-ray powder diffraction data using a recently developed direct-space (DS) methodology based on local least-squares (LS) minimizations and implemented in the program TALP (Vallcorba *et al.*, 2012b). DS methods (Cerný and Favre-Nicolin, 2007) are very powerful for solving organic compounds but require their chemical structure to be previously determined or confirmed by other techniques (e.g. NMR). In addition, both compounds contain three aromatic rings of well-known geometry. This information can be introduced to increase the precision of the initial molecular model for DS methods. As a counterpart, these systems usually give rise to powders with marked preferred orientation (PO) affecting the measured powder diffraction data. Even with moderate PO, DS methods can solve crystal structures. However, PO effect should be minimized for a proper refinement of the structures, e.g. by measuring in transmission geometry (Figure 2).

II. EXPERIMENTAL

A. General methods

Melting points were determined on a Kofler heated stage and are uncorrected. NMR spectra were recorded on a Bruker AC300 MHz in $CDCl_3$ as solvent. The system used was high-resolution mass spectrometry (HRMS) electron impact (EI) quadrupole time of flight (QqTOF) 5600 system (Applied Biosystems-MDS Sciex). Mode positive. Conditions: Gas1 35 psi, GS2: 35, CUR: 25, temperature: 450 °C, ion spray voltage: 5500 V and collision energy: 25–35 V. IR spectra were recorded using a Thermoscientific Nicolet FT IR iS10. All reactives used are from commercial sources (Aldrich). 3-Phenyl-[1,2,3]triazolo[1,5-*a*]pyridine **1a** (Boyer and Goebel, 1960) and 3-(2-pyridyl)-[1,2,3]triazolo-[1,5-*a*]pyridine **1b** (Battaglia *et al.*, 1994; Abarca *et al.*, 1998) were prepared as described elsewhere.

B. Synthesis of 3-phenyl-7-(pyrazin-2-yl)-[1,2,3]triazolo [1,5-*a*]pyridine (2)

At −40 °C, butyllithium (2.2 ml, 1.1 eq) in hexane (1.3 M) was added dropwise to a stirred solution of 3-phenyl-[1,2,3]triazolo[1,5-*a*]pyridine **1a** (0.5 g, 2.56 mmol) in toluene (50 ml). After 30 min a solution of pyrazine (0.62 g, 7.7 mmol, 3 eq) in toluene (5 ml) was added dropwise to the reaction mixture, and was allowed to react for 2 h. Then the solution was allowed to reach room temperature and a solution of $KMnO_4$ (0.4 g, 2.81 mmol, 1.1 eq) in 50 ml of water was added. After 30 min the organic layer was decanted, filtered with celite, and separated. The aqueous layer extracted with dichloromethane (3 × 50 ml). The combined organic layers were dried over sodium sulfate, filtered, and evaporated. The crude was purified by chromatotron (ethyl acetate/hexane

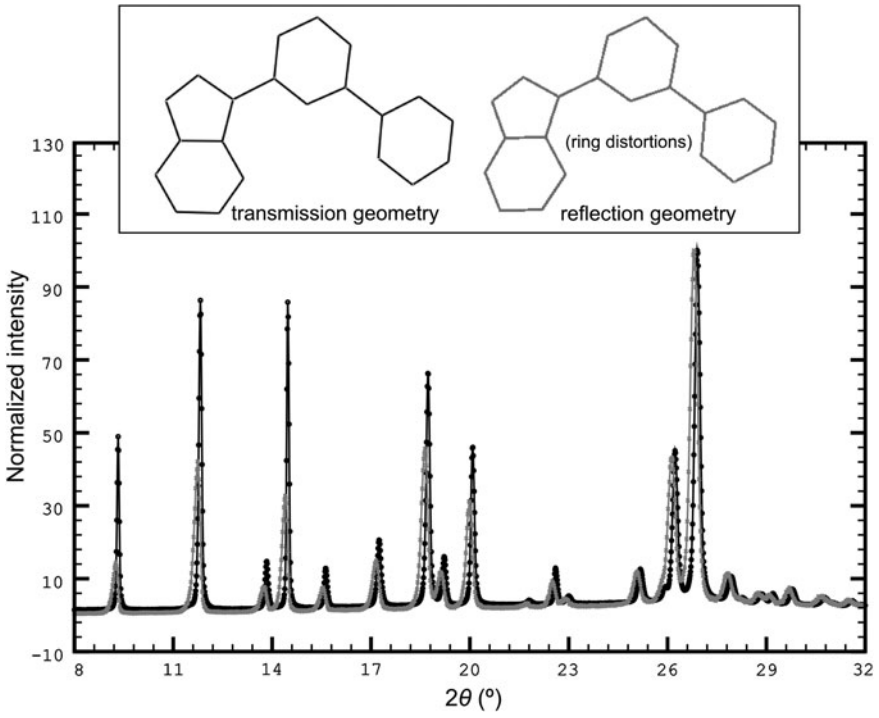

Figure 2. Laboratory powder diffraction data of **4** collected in reflection Bragg–Brentano (gray pattern) and transmission Debye–Scherrer (black pattern) geometries (Cu$K\alpha_{1,2}$ radiation) with the respective refined crystal structures (top). The Rietveld refinement from reflection geometry data results in slightly distorted atomic rings and a higher residual value ($R_{wp} = 0.102$; $\chi = 2.64$) than the structure obtained from transmission geometry data ($R_{wp} = 0.055$; $\chi = 1.41$).

https://doi.org/10.1017/S0885715614000402 Published online by Cambridge University Press

from 1:5 to 1:1) affording 3-phenyl-7-(pyrazin-2-yl)-[1,2,3]triazolo[1,5-*a*]pyridine 2 as a colorless solid (0.42 mg, 61%). Mp: 141–142 °C. ^{1}H NMR (300 MHz, $CDCl_3$): δ = 10.32 (d, J = 0.9 Hz, 1H), 8.78–8.72 (m, 2H), 8.15 (dd, J = 8.8, 0.9 Hz, 1H), 8.02–7.99 (m, 3H), 7.58–7.43 (m, 4H). ^{13}C NMR (75 MHz, $CDCl_3$): δ = 146.3 (CH), 145.4 (C), 145.3 (CH), 144.5 (CH), 138.8 (C), 134.6 (C), 131.9 (C), 131.3 (C), 129.2 (CH), 128.4 (CH), 127.2 (CH), 126.0 (CH), 119.5 (CH), 117.8 (CH). MS (EI): m/z(%) = 245 (54), 218 (13), 191 (13), 167 (100), 139 (3). HRMS for $C_{16}H_{12}N_5(M^+ + 1)$: 274.1087, found: 274.1086. IR (neat, cm^{-1}): 3108, 3031, 1540, 1458, 1394, 1264, 1127, 1058, 998, 918, 853, 722, 689.

C. Synthesis of 3-[6-(pyridazin-3-yl)-pyridin-2-yl]-[1,2,3]triazolo[1,5-*a*]pyridine (4)

At −40 °C, butyllithium (2.2 ml, 1.1 eq) in hexane (1.3 M) was added dropwise to a stirred solution of 3-(2-pyridyl)-[1,2,3]triazolo[1,5-*a*]pyridine **1b** (0.5 g, 2.55 mmol) in toluene (50 ml). After 30 min a solution of pyridazine (0.62 g, 7.7 mmol, 3 eq) in toluene (5 ml) was added dropwise to the reaction mixture, and was allowed to react for 2 h. Then the solution was allowed to reach room temperature and a solution of $KMnO_4$ (0.4 g, 2.81 mmol, 1.1 eq) in 50 ml of water was added. After 30 min the organic layer was decanted, filtered with celite, and separated. The aqueous layer was extracted with dichloromethane (3 × 50 ml). The combined organic layers were dried over sodium sulfate, filtered, and evaporated. The crude was purified by chromatotron (ethyl acetate/hexane from 1:5 to 1:1) affording 3-[6-(pyridazin-3-yl)pyridin-2-yl]-[1,2,3]triazolo[1,5-*a*]pyridine 4 (0.140 mg, 20%). Mp: 232–233 °C (AcOEt). ^{1}H NMR (300 MHz, $CDCl_3$): δ = 9.26 (dd, J = 4.9, 1.7 Hz, 1H), 8.81 (ddd, J = 7.0, 1.0, 1.0 Hz, 1H), 8.69 (ddd, J = 8.9, 1.2, 1.2 Hz, 1H), 8.63 (dd, J = 7.8, 1.0 Hz, 1H), 8.60 (dd, J = 8.5, 1.7 Hz, 1H), 8.49 (dd, J = 7.9, 1.0 Hz, 1H), 8.01 (dd, J = 7.9, 7.9 Hz, 1H), 7.69 (dd, J = 8.6, 4.9 Hz, 1H), 7.45 (ddd, J = 8.9, 6.7, 1.0 Hz, 1H), 7.10 (ddd, J = 6.9, 6.9, 1.3 Hz, 1H). ^{13}C NMR (75 MHz, $CDCl_3$): δ = 159.0 (C), 153.2 (C), 152.0 (C), 151.3 (CH), 138.2 (CH), 137.3 (C), 132.1 (C), 127.2 (CH), 126.8 (CH), 125.7 (CH), 124.4 (CH), 121.9 (CH), 120.8 (CH), 120.3 (CH), 116.0 (CH). MS (EI): m/z (%) = 247 (100), 230 (5), 220 (22), 193 (55), 167 (56), 140 (9). HRMS for $C_{15}H_{11}N_6$ $(M^+ + 1)$: 275.1040, found: 275.1037. IR (neat, cm^{-1}): 3086, 3025, 1529, 1438, 1402, 1368, 1113, 1035, 741, 691.

D. Powder X-ray diffraction

Diffraction data of **2** and **4** were collected at room temperature on a PANalytical X'Pert PRO MPD diffractometer (45 kV/40 mA, Cu$K\alpha_{1,2}$ radiation, PIXcel multistrip detector with an active detection length of 3.347°) in transmission geometry using a convergent beam with a focalizing mirror. The specimens were loaded into a 0.7 mm Lindemann glass capillary and the patterns were measured from 2.0° to 70.0° (2θ) in steps of 0.013° at 700 s per step (six consecutive scans were done).

The diffraction patterns were indexed using DICVOL04 (Boultif and Louër, 2004) with figures of merit of M_{20} = 49.5 and F_{20} = 103.8 (0.0044, 44) for **2** and M_{20} = 31.0 and F_{20} = 71.9 (0.0043, 65) for **4**. The whole-pattern matching and intensity extraction were performed with DAjust software (Vallcorba *et al.*, 2012a) and the intensities were introduced in TALP (Vallcorba *et al.*, 2012b) for structure solution. Finally, the candidate solution underwent a final restrained Rietveld refinement with RIBOLS (Rius, 2013) using all the profile points and with C–H distances fixed at 0.93 Å and refined as rigid bodies (CH) in the final refinement cycles. Crystallographic data and refinement details for both compounds are summarized in Table I.

III. RESULTS AND DISCUSSION

The crystal structure of **4** (Figure 3) is planar, with the highest dihedral angle, 7.0(3)°, between the triazolopyridine (TAP) and the pyridine (PY) rings. This planar arrangement leads to a molecular stacking along ***a*** (Figure 4) controlled by two moderate π–π interactions. The first one (A, Figure 4) is between two adjacent triazolo rings (symm. op. $-1/2 + x$, $1/2 - y$, z), showing a distance between the five-membered-ring centroids of 3.573(4) Å, a dihedral angle of 3° between ring planes and angles of 17.8° and 16.2° between the centroid–centroid vector and the normal vector to the ring planes. The second π-stacking system (B, Figure 4) is between the PD rings (symm. op. $-1/2 + x$, $1/2 - y$, z) with a distance between the six-membered-ring centroids of 3.587(4) Å, a dihedral angle of 8° between ring planes and angles of 20.8° and 16.7° between the centroid–centroid vector and the normal vector to the ring planes. Besides these π–π interactions, the N atoms also interact weakly with the neighboring molecules via C–H···N electrostatic interactions (Table II).

The crystal structure of **2** (Figure 3) is also planar with the exception of the phenyl (PH) ring that is slightly rotated by 32 (1)°. The crystal packing can be described as *zigzag* molecular layers propagating along ***a*** (Figure 5) with the rotated PH ring in the twist positions. These layers are stacked along ***c*** but in this case there is only a weak π–π interaction between the triazolo ring of the TAP and a PZ ring of a neighbor molecule (symm. op. x, $1/2 - y$, $1/2 + z$), with a distance between ring centroids of 3.791(3) Å, a dihedral angle of 9.4(3)° between

TABLE I. Crystallographic data and refinement details for **2** and **4**.

	2	4
Molecular formula	$C_{16}H_{11}N_5$	$C_{15}H_{10}N_6$
Formula weight	273.29	274.28
Crystal system	Orthorhombic	Orthorhombic
Space group	*Pbca*	$Pna2_1$
a (Å)	23.6216(3)	7.0678(1)
b (Å)	12.3664(2)	14.9426(6)
c (Å)	9.1739(1)	12.2137(4)
Volume (Å^3)	2679.83(6)	1289.91(7)
Z	8	4
Calculated density (g/cm^3)	1.355	1.412
Rietveld refinement details		
Radiation	Cu$K\alpha_{1,2}$	Cu$K\alpha_{1,2}$
Profile function	Pseudo-Voigt	Pseudo-Voigt
2θ range used (°)	6.039–69.024	6.039–69.024
No. of reflections	559	287
Data points	4845	4845
Parameters	74	77
Restraints	82	82
R_{wp}	0.045	0.055
Goodness of fit (χ)	1.091	1.413

https://doi.org/10.1017/S0885715614000402 Published online by Cambridge University Press

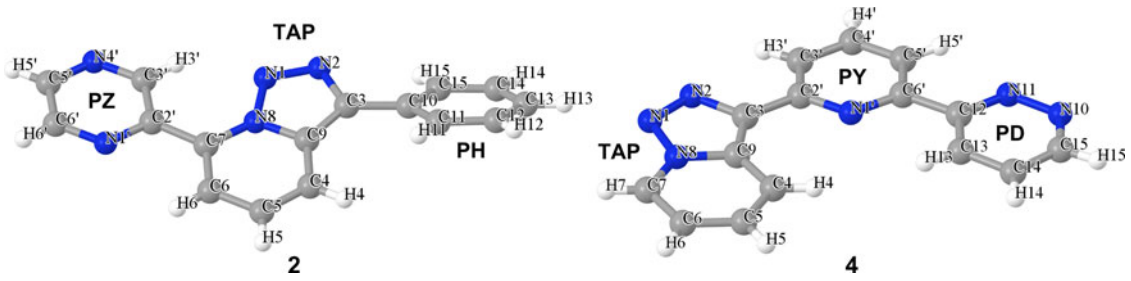

Figure 3. (Color online) Crystal structure of **2** and **4** with the atom numbering and ring acronyms: triazolopyridine (TAP), pyridine (PY), pyradizine (PD), pyrazine (PZ), and phenyl (PH) rings.

ring planes and angles of 23.6° and 23.5° between the centroid–centroid vector and the normal vector to the ring planes. Weak C–H···N intermolecular electrostatic interactions are also present, all of them occurring between molecules of the same layer and along the *b* direction (Table II).

The C–H···N intermolecular electrostatic interactions observed in **2** and **4** are weak but important for the crystal packing of these organic compounds (Thalladi *et al.*, 2000). The H···N distances range from 2.48 to 2.73 Å (sum of Van der Waals radius = 2.75 Å) and the C–H···N angles are comprised between 120° and 180° (Table II) as expected for these types of interactions (Mascal, 1998).

In both structures, the six-membered rings that contain N atoms (PD, PZ) can be rotated by 180° keeping the overall geometry of the structure. However, this rotation affects the relative position of two N atoms and two H atoms in each ring. The small difference between the C and N X-ray scattering powers and the small contribution of the two H atoms complicates the determination of the ring conformation from powder diffraction data. In the case of **4**, the rotation of the PD ring results in two close H atoms (H13 and H5′) and the ring would have to be slightly rotated to avoid this short contact. A refinement of the structure starting from the 180° rotated PD ring leads to a $\chi = 1.48$, which is slightly higher than the previous one (1.41). In spite of the small difference between these two possible ring orientations, powder diffraction data clearly show a better agreement with the chemically less hindered one. The case of **2** is similar, because a rotation of the PZ ring could be also possible (despite the short distance between H3′ and H6); however, this alternative refinement is also worse compared with the previous one ($\Delta\chi = 0.1$).

IV. CONCLUSION

The crystal structures of two novel substituted triazolopyridines have been completely determined from laboratory powder X-ray diffraction data. The crystal packing is clearly characterized by π–π interactions in **4** and weak intermolecular C–H···N interactions play an important role in the crystal structure packing of both the compounds. The conformations of the six-membered rings determined from powder data correspond to the ones that are less sterically hindered. However, when

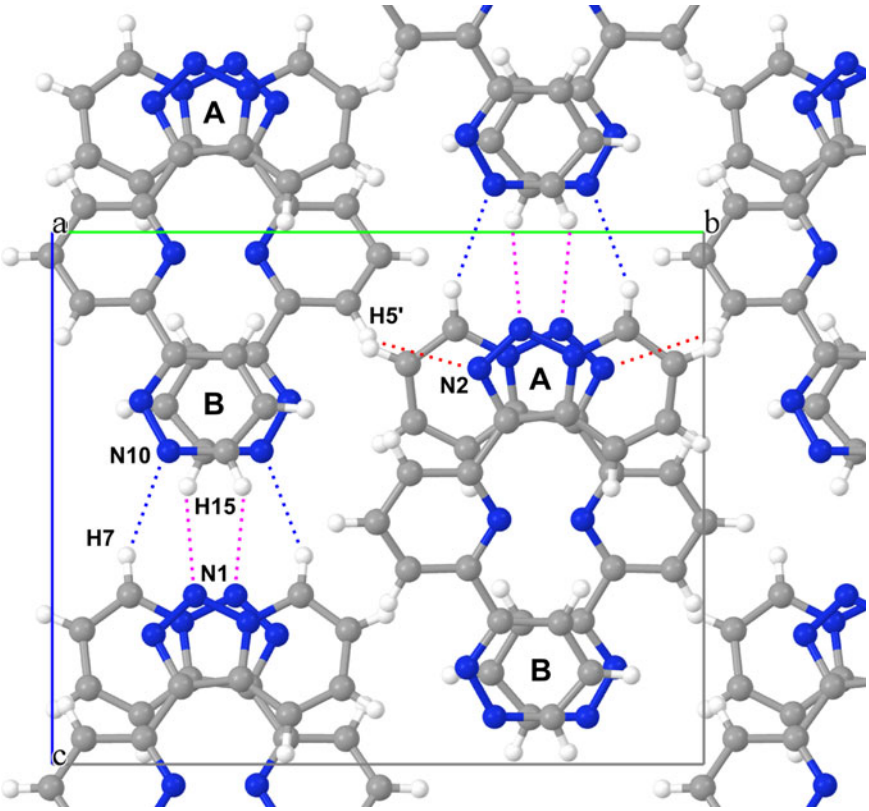

Figure 4. (Color online) Crystal structure packing of **4** projected along *a* direction showing the two systems of π–π interactions (A and B) and the three weak C–H···N interactions.

https://doi.org/10.1017/S0885715614000402 Published online by Cambridge University Press

TABLE II. Summary of C–H···N interactions in crystal structures **2** and **4**.

Molec.	Atoms	H···N distance (Å)	C–H···N angle (°)	C···N distance (Å)
2	C6′–H6′···N1	2.648(6)	147.2(4)	3.466(9)
2	C6′–H6′···N2	2.589(5)	160.9(4)	3.481(8)
2	C6–H6···N4′	2.487(5)	148.5(3)	3.316(8)
4	C7–H7···N10	2.707(6)	154.6(4)	3.570(8)
4	C15–H15···N1	2.574(5)	152.3(5)	3.425(7)
4	C5′–H5′···N2	2.728(7)	128.8(4)	3.390(10)

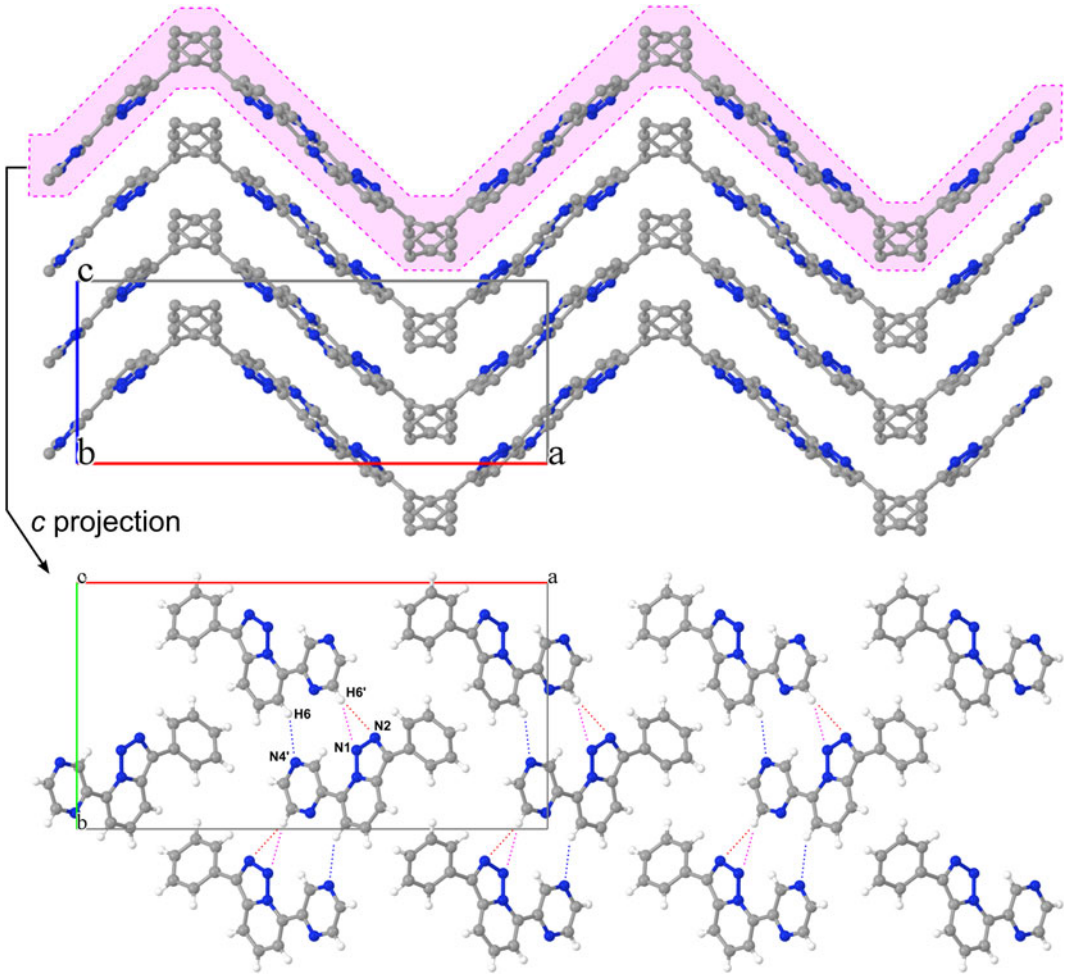

Figure 5. (Color online) Crystal structure packing of **2** projected along ***b*** showing the *zigzag* layers of molecules and (bottom) the projection along ***c*** of one of the layers showing the weak C–H···N intralayer interactions.

coordinated to a metal these conformations change in order to face the N atoms to the metal atom resulting in a small planar distortion of the rings (Ramírez de Arellano *et al.*, 2013).

The DS strategy implemented in TALP can solve crystal structures of organic compounds from powders. TALP can use powder data affected by a certain degree of PO of the sample but, for later refinements, it is better to minimize these orientation effects during the powder data collection (i.e. using transmission geometry).

ACKNOWLEDGEMENTS

The authors thank the Ministerio de Economia y Competitividad (Project Nos. MAT2009-07967, MAT2012-35-35247, Consolider NANOSELECT CSD2007-00041, CONSOLIDER-INGENIO SUPRAMED CSD 2010-00065), the Generalitat de Catalunya (SGR2009), and Generalitat Valenciana (Valencia, Spain) (Project PROMETEO 2011/008) for the financal support. O.V. also acknowledges NANOSELECT for a contract. R.A. thanks Generalitat Valenciana for a doctoral fellowship. The transmission XRPD patterns were collected at the CCiT of University of Barcelona and the realization of HRMS spectra was carried out in SCSIE (University of Valencia).

SUPPLEMENTARY MATERIAL

The supplementary material for this article can be found at http://www.journals.cambridge.org/PDJ

Abarca, B., Ballesteros, R., and Elmasnaouy, M. (**1998**). "A facile route to new potential helicating ligands," Tetrahedron **54**, 15287–15292.

https://doi.org/10.1017/S0885715614000402 Published online by Cambridge University Press

Abarca, B., Ballesteros, R., and Chadlaoui, M. (**2004**). "Triazolopyridines. Part 24: new polynitrogenated potential helicating ligands," Tetrahedron **60**, 5785–5792.

Abarca, B., Alkorta, I., Ballesteros, R., Blanco, F., Chadlaoui, M., Elguero, J., and Mojarrad, F. (**2005**). "3-(2-Pyridyl)-[1,2,3]triazolo [1,5-a]pyridines. An experimental and theoretical (DFT) study of the ring–chain isomerization," Org. Biomol. Chem. **3**, 3905–3910.

Abarca, B., Aucejo, R., Ballesteros, R., Blanco, F., and García-España, E. (**2006**). "Synthesis of novel fluorescent 3-aryl-and 3-methyl-7-aryl-[1,2,3]triazolo[1,5-a] pyridines by Suzuki cross-coupling reactions," Tetrahedron Lett. **47**, 8101–8103.

Adam, R., Ballesteros-Garrido, R., Vallcorba, O., Abarca, B., Ballesteros, R., Leroux, F. R., Colobert, F., Amigó, J. M., and Rius, J. (**2013**). "Synthesis and structural properties of an hexaaza[5]helicene containing two [1,2,3]triazolo[1,5-a]pyridine moieties," Tetrahedron Lett. **54**, 4316–4319.

Arcís-Castillo, Z., Piñeiro-López, L., Muñoz, M. C., Ballesteros, R., Abarca, B., and Real, J. A. (**2013**). "Structural, magnetic and calorimetric studies of a crystalline phase of the spin crossover compound $[Fe(tzpy)_2(NCSe)_2]$," CrystEngComm **15**, 3455–3462.

Ballesteros, R., Abarca, B., Samadi, A., Server-Carrió, J., and Escrivà, E. (**1999**). "Coordinating behaviour of 3-methyl[1,2,3]triazolo[1,5-a]pyridine (tzpy): crystal and molecular structure and electronic properties of $[Cu(tzpy)_2(ONO_2)_2(OH_2)]$," Polyhedron **18**, 3129–3133.

Ballesteros-Garrido, R., Abarca, B., Ballesteros, R., de Arellano, C. R., Leroux, F. R., Colobert, F., and García-España, E. (**2009**). "[1,2,3] Triazolo[1,5-a]pyridine derivatives as molecular chemosensors for zinc (II), nitrite and cyanide anions," New J. Chem. **33**, 2102–2106.

Ballesteros-Garrido, R., Delgado-Pinar, E., Abarca, B., Ballesteros, R., Leroux, F. R., Colobert, F., Zaragozá, R. J., and García-España, E. (**2012**). "Triazolopyridines. Part 28. The ring–chain isomerization strategy: triazolopyridine- and triazoloquinoline–pyridine based fluorescence ligands," Tetrahedron **68**, 3701–3707.

Battaglia, L. P., Carcelli, M., Ferraro, F., Mavilla, L., Pelizzi, C., and Pelizzi, G. (**1994**). A convenient method for the preparation of 3-(2-pyridyl) triazolo[1,5-a]pyridine (L). Crystal structures of L and $[CuL_2(OH_2)_2][NO_3]_2$," J. Chem. Soc., Dalton Trans. **1994**, 2651–2654.

Boultif, A. and Louër, D. (**2004**). "Powder pattern indexing with the dichotomy method," J. Appl. Crystallogr. **37**, 724–731.

Boyer, J. and Goebel, N. (**1960**). "The identification of $C_{12}H_8N_4O$, an oxidation product from α-pyridil monohydrazone," J. Org. Chem. **25**, 304–305.

Cerný, R. and Favre-Nicolin, V. (**2007**). "Direct space methods of structure determination from powder diffraction: principles, guidelines and perspectives," Z. Kristallogr. **222**, 105–113.

Chadlaoui, M., Abarca, B., Ballesteros, R., Ramírez de Arellano, C., Aguilar, J., Aucejo, R., and García-España, E. (**2006**). "Properties of a triazolopyridine system as a molecular chemosensor for metal ions, anions, and amino acids," J. Org. Chem. **71**, 9030–9034.

Jones, G. and Abarca, B. (**2010**). "The chemistry of the [1,2,3]triazolo[1,5-a] pyridines: an update," Adv. Heterocycl. Chem. **100**, 195–252.

Jones, G. and Sliskovic, D. R. (**1980**). "[1,2,3]Triazolo[1,5-a]pyridine-a synthon for 6-substituted pyridine-2-carboxaldehydes," Tetrahedron Lett. **21**, 4529–4530.

Jones, G. and Sliskovic, D. R. (**1982**). "Triazolopyridines. Part 2. Preparation of 7-substituted triazolo[1,5-a]pyridines by directed lithiation," J. Chem. Soc., Perkin Trans. **1**, 967–971.

Jones, G., Mouat, D. J., and Tonkinson, D. J. (**1985**). "Triazolopyridines. Part 6. Ring opening reactions of triazolopyridines," J. Chem. Soc., Perkin Trans. **1**, 2719–2723.

Jones, G., Pitman, M. A., Lunt, E., Lythgoe, D. J., Abarca, B., Ballesteros, R., and Elmasnaouy, M. (**1997**). "Triazolopyridines. 18. Nucleophilic substitution reactions on triazolopyridines; a new route to 2, 2′-bipyridines," Tetrahedron **53**, 8257–8268.

Kress, T. J. (**1979**). "Direct metalation of pyrimidine. Synthesis of some 4-substituted pyrimidines," J. Org. Chem. **44**, 2081–2082.

Mascal, M. (**1998**). "Statistical analysis of C–H···N hydrogen bonds in the solid state: there are real precedents," Chem. Commun. **1998**, 303–304.

Niel, V., Gaspar, A. B., Muñoz, M. C., Abarca, B., Ballesteros, R., and Real, J. A. (**2003**). "Spin crossover behavior in the iron (II)-2-pyridyl[1,2,3]triazolo[1,5-a]pyridine system: X-ray structure, calorimetric, magnetic, and photomagnetic studies," Inorg. Chem. **42**, 4782–4788.

Ramírez de Arellano, C., Escrivà, E., Gómez-García, C. J., Mínguez Espallargas, G., Ballesteros, R., and Abarca, B. (**2013**). "Hydrogen bonding versus π-stacking in ferromagnetic interactions. Studies on a copper triazolopyridine complex," CrystEngComm **15**, 1836–1839.

Rius, J. (**2013**). *RIBOLS: Least-Squares Refinement from Powder Diffraction Data*, version 1310 (Computer Software) (Institut de Ciència de Materials de Barcelona (ICMAB-CSIC), Barcelona, Spain).

Thalladi, V. R., Gehrke, A., and Boese, R. (**2000**). "C–H group acidity and the nature of C–H···N interactions: crystal structural analysis of pyrazine and methyl substituted pyrazines," New J. Chem. **24**, 463–470.

Vallcorba, O., Rius, J., Frontera, C., Peral, I., and Miravitlles, C. (**2012a**). "DAJUST: a suite of computer programs for pattern matching, space-group determination and intensity extraction from powder diffraction data," J. Appl. Crystallogr. **45**, 844–848.

Vallcorba, O., Rius, J., Frontera, C., and Miravitlles, C. (**2012b**). "TALP: a multisolution direct-space strategy for solving molecular crystals from powder diffraction data based on restrained least squares," J. Appl. Crystallogr. **45**, 1270–1277.